

Supporting Information

Innovative InAg-Carbon Nanocomposites: Mesoporous Design forOER Enhancement

Sandhyawasini Kumari,^{a,b#} Somnath C. Dhawale,^{c#} Afaq Ahmad Khan,^{*d} Hanumant B. Kale,^e Bhaskar R. Sathe,^c Manoj B. Gawande,^{*e,f} and M.S. Santosh^{*a,b}

^a*Coal to Hydrogen Energy for Sustainable Solutions (CHESS) Division, CSIR – Central Institute of Mining and Fuel Research (CIMFR), Digwadih Campus, PO: FRI, Dhanbad – 828108, Jharkhand, India.*

^b*Academy of Scientific and Innovative Research (AcSIR), Ghaziabad 201 002, India.*

^c*Department of Chemistry, Dr. Babasaheb Ambedkar Marathwada University Chhatrapati Sambhajinagar 431004 (MS) India.*

^d*GreenCat Laboratory, Department of Chemical Engineering, Indian Institute of Technology (Indian School of Mines) Dhanbad-826004 (India).*

^e*Department of Industrial and Engineering Chemistry, Institute of Chemical Technology, Mumbai-Marathwada Campus, Jalna-431213 Maharashtra, India.*

^f*Centre for Energy and Environmental Technologies (CEET), Nanotechnology Centre, VŠB–Technical University of Ostrava, 17. listopadu 2172/15, 708 00 Ostrava-Poruba, Czech Republic.*

***Corresponding Authors:** M.S. Santosh (santoshms@cimfr.res.in); M. B. Gawande, (mb.gawande@marj.ictmumbai.edu.in); Afaq Ahmad Khan (afaq625@gmail.com)

#- Both authors contributed equally

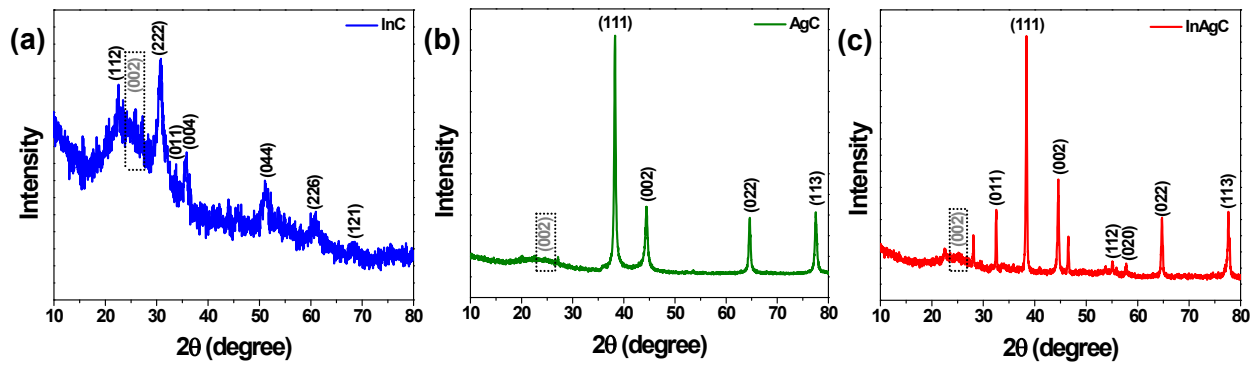


Fig. S1 Powder-XRD patterns of synthesized (a) InC, (b) AgC, and (c) InAgC nanocomposite catalyst with indicated (002) peak in bracket of graphitic carbon (C_1).

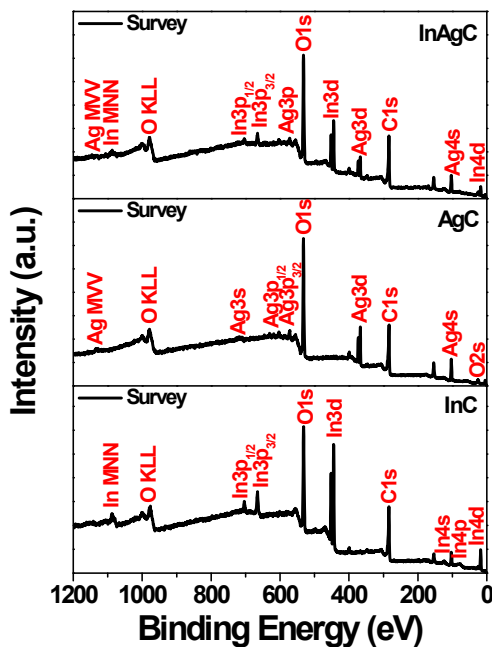


Fig. S2 Survey XPS spectra of InC, AgC, and InAgC nanocomposites.

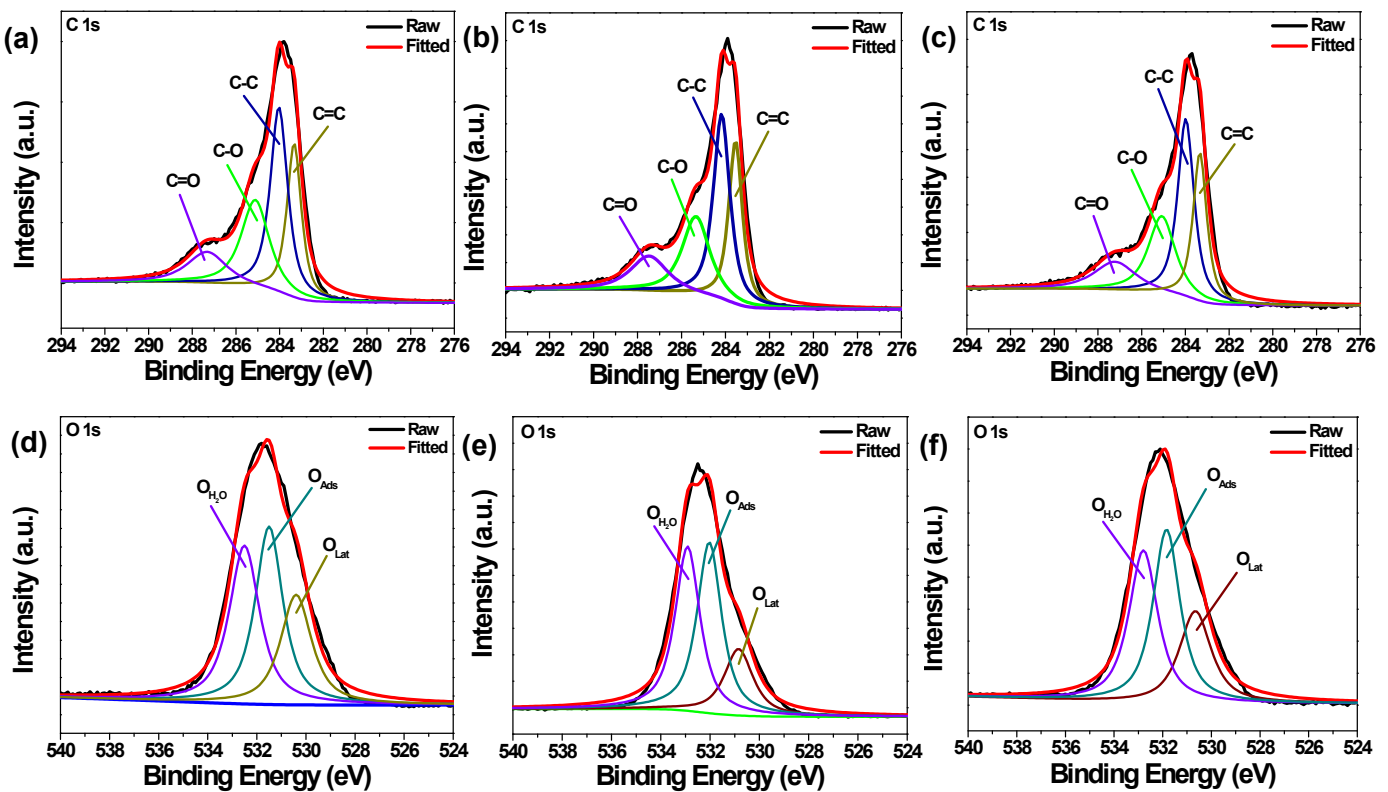


Fig. S3 High-resolution XPS spectra:(a) C 1s of InC, (b) C 1s of AgC, (c) C 1s of InAgC, (d) O 1s of InC, (e) O 1s of AgC, and (f) O 1s of InAgC.

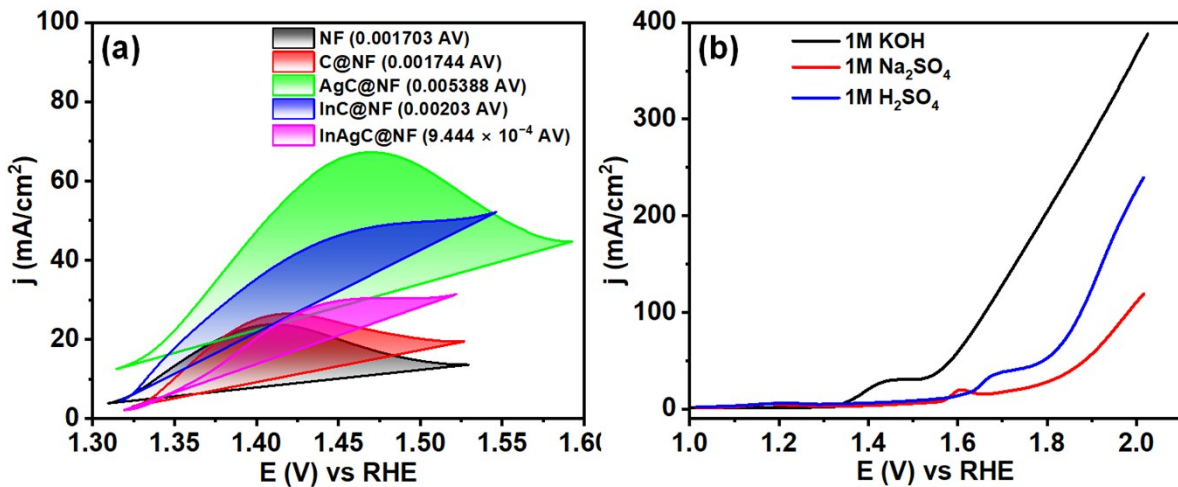


Fig. S4 (a) The isolated oxidation peaks of the same LSVs used for charge integration and the calculation of the number of active sites of C@NF, AgC@NF, InC@NF, and InAgC@NF, (b) electrolyte-dependant OER study of InAgC@NF.

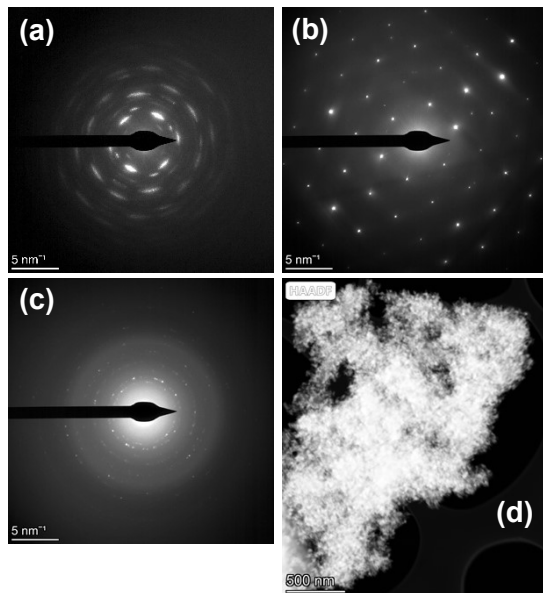


Fig. S5 SAED pattern of (a) InC, (b) AgC, (c) InAgC, and (d) HAADF image of InAgC

Table S1: Specific surface area (S_{BET}), pore width, and pore volume of the prepared catalysts

Catalyst	S_{BET} ($m^2 \cdot g^{-1}$)	Pore width (nm)	Pore volume ($cm^3 \cdot g^{-1}$)
InC	31.5	1.9	0.203
AgC	43.8	3.4	0.146
InAgC	38.4	3.1	0.127

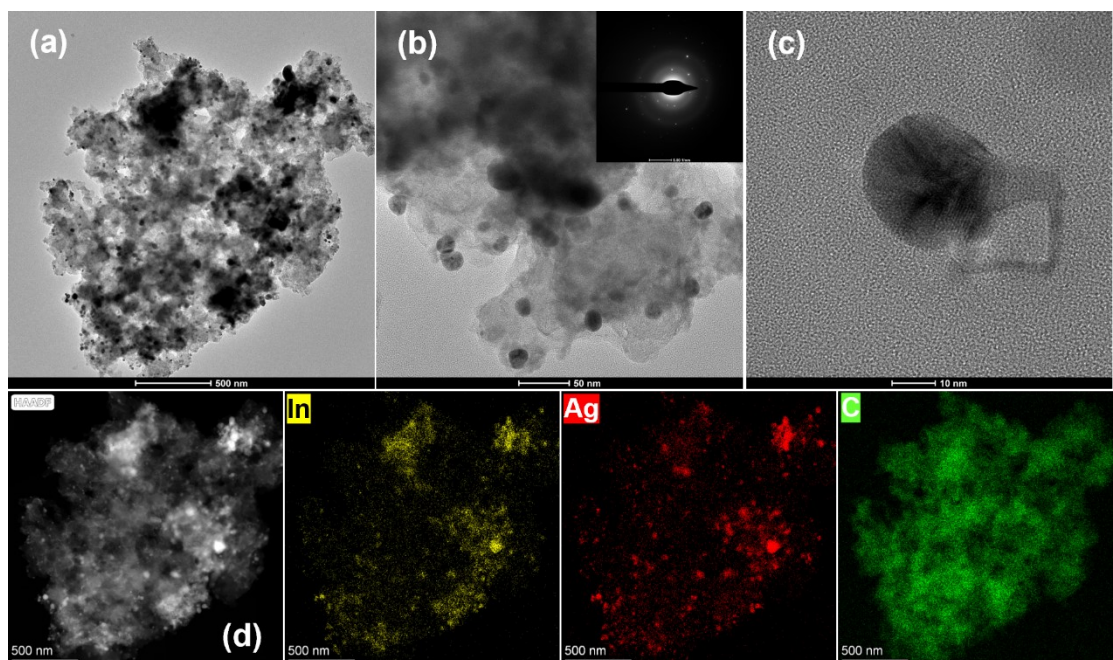


Fig. S6 (a-b) TEM micrographs with inset SAED pattern, (c) HR-TEM micrographs, (d) STEM-EDS mapping of InAgC nanocomposite after catalytic process.

Table S2: OER activity comparison table with reported OER catalysts (mono, bi and trimetallic catalysts).

Catalyst	Composition	Electrode	Overpotential (V)	Tafel Slope (mV/dec)	Current Density (mA/cm ²)	Reference
Fe ₂ O ₃	Monometallic	Ti foil substrate	0.65	56	10	[1]
MnO ₂	Monometallic	FTO substrate	0.48	79	10	[2]
Ni ₂ Ta	Bimetallic	PVC-coated Sn-plated copper wire	0.57	167	10	[3]
Ni ₄₀ Fe ₄₀ P ₂₀	Trimetallic	glass carbon electrode	0.54	40	10	[4]
Ag-Co ₃ O ₄	Bimetallic	FTO substrate	0.68	219	10	[5]
Ag-doped CoOOH	Bimetallic	Polycrystalline gold, silver, copper and nickel thin films	0.256	64.6	10	[6]
Ag/Co(OH) ₂	Bimetallic	Carbon paper	0.283	97	10	[7]
Ag-CoFe@NC	Trimetallic	Carbon layer	0.320	109	10	[8]
In-doped Fe-COF	Bimetallic	Ni foam	0.28	53	50	[9]
In/C	Monometallic	Ni foam	0.49	110	100	This work
Ag/C	Monometallic	Ni foam	0.61	127	100	
In/Ag/C	Bimetallic	Ni foam	0.48	97	100	

References

1. Kwong, W. L.; Lee, C. C.; Shchukarev, A.; Björn, E.; Messinger, J., High-performance iron (III) oxide electrocatalyst for water oxidation in strongly acidic media. *Journal of Catalysis* **2018**, 365, 29-35.
2. Li, A.; Ooka, H.; Bonnet, N.; Hayashi, T.; Sun, Y.; Jiang, Q.; Li, C.; Han, H.; Nakamura, R., Stable potential windows for long-term electrocatalysis by manganese oxides under acidic conditions. *Angewandte Chemie* **2019**, 131 (15), 5108-5112.
3. Mondschein, J. S.; Kumar, K.; Holder, C. F.; Seth, K.; Kim, H.; Schaak, R. E., Intermetallic Ni₂Ta electrocatalyst for the oxygen evolution reaction in highly acidic electrolytes. *Inorganic chemistry* **2018**, 57 (10), 6010-6015.
4. Hu, F.; Zhu, S.; Chen, S.; Li, Y.; Ma, L.; Wu, T.; Zhang, Y.; Wang, C.; Liu, C.; Yang, X., Amorphous metallic NiFeP: a conductive bulk material achieving high

activity for oxygen evolution reaction in both alkaline and acidic media. *Advanced Materials* **2017**, *29* (32), 1606570.

5. Yan, K.-L.; Chi, J.-Q.; Xie, J.-Y.; Dong, B.; Liu, Z.-Z.; Gao, W.-K.; Lin, J.-H.; Chai, Y.-M.; Liu, C.-G., Mesoporous Ag-doped Co₃O₄ nanowire arrays supported on FTO as efficient electrocatalysts for oxygen evolution reaction in acidic media. *Renewable Energy* **2018**, *119*, 54-61.
6. Lee, C.; Shin, K.; Jung, C.; Choi, P.-P.; Henkelman, G.; Lee, H. M., Atomically embedded Ag via electrodiffusion boosts oxygen evolution of CoOOH nanosheet arrays. *ACS Catalysis* **2019**, *10* (1), 562-569.
7. Guo, W.; Kim, J.; Kim, H.; Han, G. H.; Jang, H. W.; Kim, S. Y.; Ahn, S. H., Sandwich-like Co (OH) x/Ag/Co (OH) 2 nanosheet composites for oxygen evolution reaction in anion exchange membrane water electrolyzer. *Journal of Alloys and Compounds* **2021**, *889*, 161674.
8. Wang, Y.; Yuan, H.; Liu, F.; Hu, T., A triphasic nanocomposite with a synergistic interfacial structure as a trifunctional catalyst toward electrochemical oxygen and hydrogen reactions. *Journal of Materials Chemistry A* **2021**, *9* (11), 7114-7121.
9. Hedau, B.; Ha, T.-J., Indium-doped iron-coordinated covalent organic framework as an efficient bifunctional oxygen electrocatalyst for energy applications. *Journal of Alloys and Compounds* **2025**, *1010*, 178134.